



Peach, J., Czajka, A., Hazell, G., Hill, C., Mohamed, A., Pegg, J. C., Rogers, S. E., & Eastoe, J. (2017). Tuning Micellar Structures in Supercritical CO₂ Using Surfactant and Amphiphile Mixtures. *Langmuir*, 33(10), 2655-2663.
<https://doi.org/10.1021/acs.langmuir.7b00324>

Peer reviewed version

Link to published version (if available):
[10.1021/acs.langmuir.7b00324](https://doi.org/10.1021/acs.langmuir.7b00324)

[Link to publication record in Explore Bristol Research](#)
PDF-document

This is the author accepted manuscript (AAM). The final published version (version of record) is available online via ACS at <https://pubs.acs.org/doi/10.1021/acs.langmuir.7b00324>. Please refer to any applicable terms of use of the publisher.

University of Bristol - Explore Bristol Research

General rights

This document is made available in accordance with publisher policies. Please cite only the published version using the reference above. Full terms of use are available:
<http://www.bristol.ac.uk/red/research-policy/pure/user-guides/ebr-terms/>

Tuning Micellar Structures in Supercritical CO₂ Using Surfactant and Amphiphile Mixtures – Supporting Information

Jocelyn Peach[†], Adam Czajka[†], Gavin Hazell[†], Christopher Hill[†], Azmi Mohamed[‡], Jonathan
C. Pegg[†], Sarah E. Rogers[§], Julian Eastoe^{*,†}

Author Address

[†] School of Chemistry, University of Bristol, Bristol, BS8 1TS, United Kingdom

[‡] University Pendidikan Sultan Idris, Faculty of Science and Mathematics, Department of
Chemistry, Tanjong Malim 35900, Perak, Malaysia.

[§] Rutherford Appleton Laboratory, ISIS Spallation Source, Chilton, Oxfordshire, OX11 0QT,
United Kingdom

Small-Angle Neutron Scattering (SANS)

SANS data have been fitted to form factors describing either spheres, ellipsoids or rods using the program SASview¹, employing an iterative, least-squares fitting process. Known model parameters, such as scattering length densities and volume fractions were set to constant values, and unknown fit parameters, such as micellar radius and background scattering, were allowed to ‘float’. The equations describing the different form factors are given below.

i. Spheres

The form factor for a sphere is Equation S 1.

$$P(Q) = \frac{Scale}{V} \left[\frac{3V(\Delta\rho)[\sin(Qr) - qr \cos(Qr)]}{(Qr)^3} \right]^2 + bkg$$

22 *Equation S 1*

23 Where scale is a factor used to put the intensity on an absolute scale, V is the scattering particle
24 volume, r is the scattering particle radius and bkg is the background incoherent scattering. In
25 the case of polydisperse spheres, r is further defined by a Schultz distribution of homogeneous
26 spheres, Equation S 2.

27
$$r = \frac{\left(\frac{Z+1}{\bar{R}}\right)^{Z+1} R^Z \left[-\frac{Z+1}{\bar{R}} R\right]}{\Gamma(Z+1)}$$

28 *Equation S 2*

29 Where R is the mean of the radius distribution and the polydispersity being defined by the RMS
30 deviation, $\sigma = R/(Z+1)^{1/2}$ where the width parameter is $Z > -1$. During the fitting process, the
31 scattering lengths and the scale have been fixed, and r, bkg and polydispersity have been
32 allowed to vary.

33 **ii. Ellipsoids**

34 The scattering from ellipsoids can be described below (Equation S 3, Equation S 4, Equation
35 S 5).

36
$$P(Q, \alpha) = \frac{scale}{V} f^2(Q) + bkg$$

37 *Equation S 3*

38
$$f(Q) = \frac{3(\Delta\rho)V(\sin[Qr(R_a R_b \alpha)] - Qr \cos[Qr(R_a R_b \alpha)])}{[Qr(R_a R_b \alpha)]}$$

39 *Equation S 4*

40
$$r(R_a R_b \alpha) = [R_b^2 \sin^2 \alpha + R_a^2 \cos^2 \alpha]^{1/2}$$

41 *Equation S 5*

42 Where α is the angle between the axis of the ellipsoid and the Q-vector, V is the ellipsoid
43 volume, R_a is the polar radius, R_b is the equatorial radius and $\Delta\rho$, the contrast, is the scattering

length density difference between the scattering ellipsoid and the solvent¹. During the fitting process, the scattering lengths and the scale have been fixed, whereas R_a , R_b , and bkg have been allowed to vary.

When $R_a > R_b$, the ellipsoid is said to be prolate, or rod-like, when $R_a = R_b$, the equations tend to a spherical form factor, and when $R_a < R_b$, the ellipsoid is said to be disk-like, or oblate. When the aspect ratio of the ellipsoid, $J_{mic} = R_a/R_b$, has the value $0.2 < 5$, an ellipsoid form factor is best employed. When the aspect ratio, has a value of $5 \leq J_{mic}$, the particle can be better considered as rod-like, and a rod-like form factor is best employed.

iii. Rods

The form factor for randomly oriented rods is given below (Equation S 6, Equation S 7).

$$P(Q, \alpha) = \frac{scale}{V} f^2(Q) + bkg$$

Equation S 6

$$f(Q) = 2(\Delta\rho) \frac{\sin(\frac{1}{2QL \cos \gamma})}{\frac{1}{2QL \cos \gamma}} \frac{J_1(Qr \sin \gamma)}{Qr \sin \gamma}$$

Equation S 7

$$V = 2\pi r^2 L$$

Equation S 8

Where V is the cylinder volume (Equation S 8), L is the cylinder length, r is the cross-sectional radius, $J_1(x)$ is the first order Bessel function of the first kind, $\Delta\rho$, the contrast, i.e. scattering length density difference between the scattering particle and the solvent. Integration is carried out over angle γ between the Q vector and the axis of the rod. During the fitting process, the scattering lengths and the scale were fixed, and L , r , and bkg were allowed to vary.

iv. Contrast Term

The strength of the interaction of the free neutrons with bound nuclei in the sample is quantified as the scattering length of the atom, b_i , an isotope dependent parameter. Scattering length density, ρ_{sld} , is the scattering length per unit volume of substance, Equation S 9;

$$\rho_{sld} = \Sigma \frac{n_i b_i}{V_m}$$

Equation S 9

where n_i is the number of nuclei of a type i , and V_m is the molecular volume. The scattering length density difference between the deuterated core of the microemulsions and the carbon dioxide solvent. Scattering length densities of the materials used in this research are given in Figure S 1.

Component	$\rho_{sld} (10^{10} \text{ cm}^{-2})$
scCO ₂ (400 bar, 318 K)	2.50
D ₂ O	6.34
TCF2	2.33
DCF2	2.19
Hybrid CF2:AOT4	1.34
Hybrid CF2:SIS1	2.13
C8benz	0.86
C2benz	1.45
DIGSS	1.16

Figure S 1 - Scattering length densities of compounds used in this research.

SANS Data

Scattering data and fits not shown in the main manuscript are presented below.

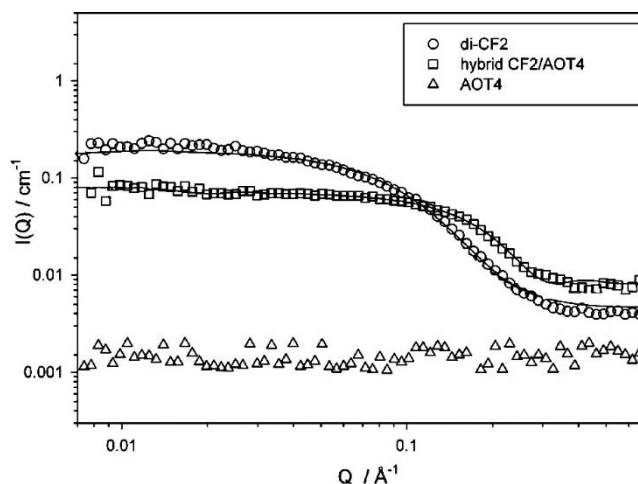


Figure S 2 - High-pressure Small-angle Neutron Scattering (HP-SANS) profiles of DCF2 and hybrid CF2:AOT4 surfactants in w/c microemulsions in the absence of hydrotrope. Model fits are to a Schultz distribution of polydisperse spheres, Radii = 15Å and 18Å respectively. Surfactant concentration = 0.05 mol dm⁻³, w = 10, T = 40°C, P = 380 bar. Reprinted from with permission from reference 2.

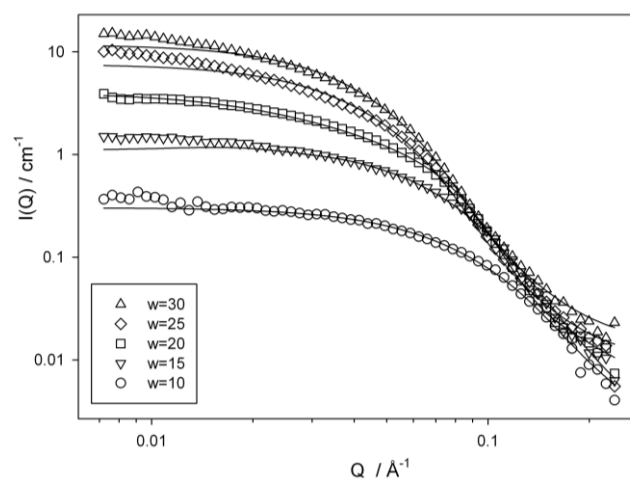
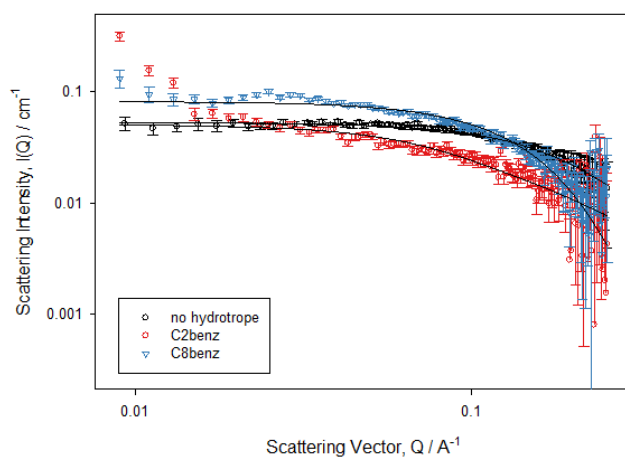


Figure S 3 - SANS profiles for various w ratios with DCF2 in pure CO₂. [Surfactant] = 0.05 mol dm⁻³, pressure = 380 bar and T = 25°C. P_{trans} @ w10 = 198 bar. Lines through data points are model fits to a Schultz distribution of polydisperse spheres. Fitted parameters are listed in Figure S 4. Reprinted with permission from ²

90

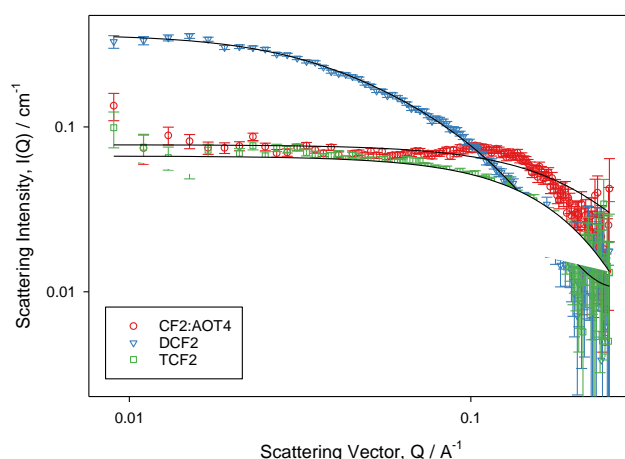
w ratio	radius $\pm 2\text{\AA}$	
	model fit	Guinier radius
10	17	15
15	19	18
20	28	25
25	32	30
30	37	33

Figure S 4 Model fits from Figure S 3, reprinted with permission from²



92

Figure S 5 - HP-SANS profile for DCF2 / water / scCO₂ microemulsions with C2benz (open spheres, red) and C8benz (open triangles, blue) hydrotrope, [surf] = 0.05 mol dm⁻³, X = 0.10, w = 5. Samples with no hydrotrope shown in open squares, black. Fits are to polydisperse sphere and ellipsoid form factor models and are displayed in the main manuscript.



96

Figure S 6 - HP-SANS profile for CO₂-philic surfactant / water / scCO₂ microemulsions with C2benz hydrotrope, [surf] = 0.05 mol dm⁻³, X = 0.10, w = 10, pressure = 350 bar, T = 45°C. Surfactant TCF2 (open squares, green), surfactant DCF2 (open triangles, blue) and hybrid surfactant CF2:AOT4 (open circles, red). Fits are to polydisperse sphere and ellipsoid form factor models and are displayed in the main manuscript.

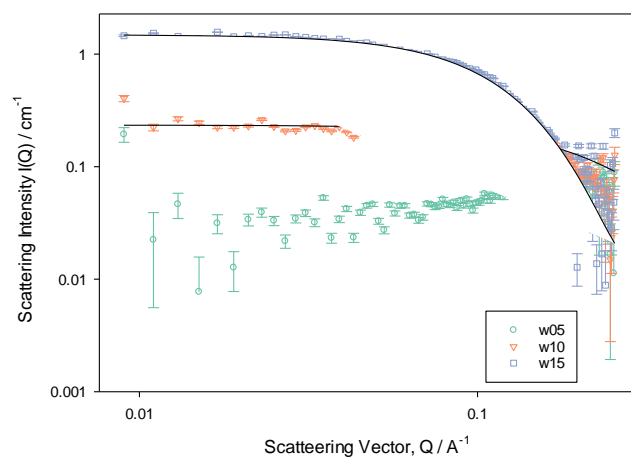


Figure S 7- HP-SANS profile for hybrid CF₂:AOT4 / water / scCO₂ microemulsions at 350 bar with c2benz hydrotrope. [surf] = 0.05 mol dm⁻³, X = 0.10, w = 5 (open circles, green), w = 10 (open triangles, orange), w = 15 (open squares, blue). Fits are to spheres and ellipsoids and are displayed in the main manuscript.

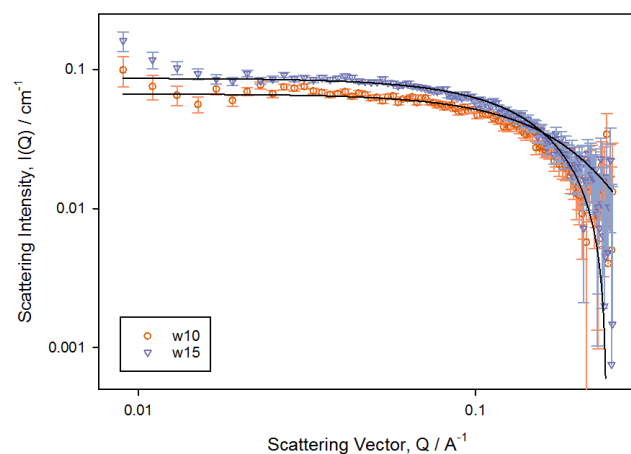
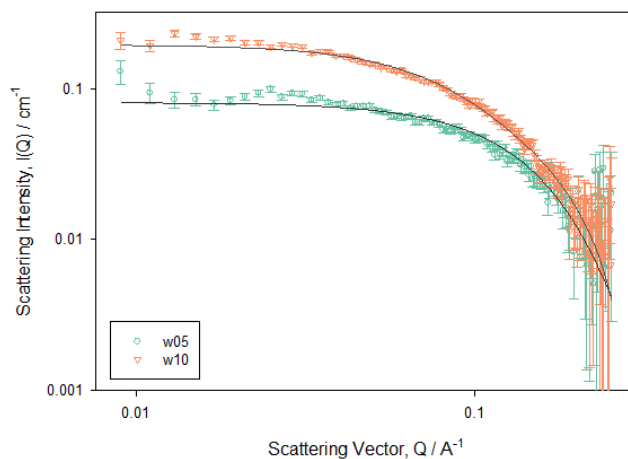


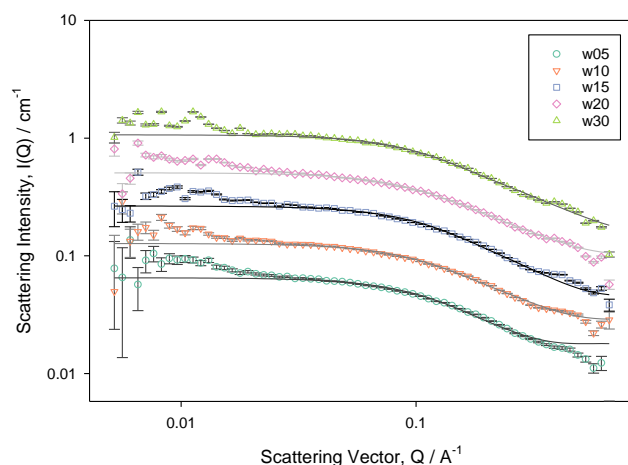
Figure S 8 - HP-SANS profile for TCF2 / water / scCO₂ microemulsions at 350 bar with c2benz hydrotrope. [surf] = 0.05 mol dm⁻³, X = 0.10, w = 10 (open spheres, orange), w = 15 (open triangles, blue). Fits are to polydisperse sphere and ellipsoid form factor models and are displayed in the main manuscript.

110



111

112 *Figure S 9 –HP-SANS profile for DCF2 / water / scCO₂ microemulsions at 350 bar with c8benz hydrotrope. [surf] = 0.05 mol*
 113 *dm⁻³, X = 0.10, w = 5 (open circles, green) and w = 10 (open triangles, orange). . Fits are to polydisperse sphere and ellipsoid*
 114 *form factor models and are displayed in the main manuscript.*



115

116 *Figure S 10 - HP-SANS profile for hybrid CF₂:AOT4 / water / scCO₂ microemulsions at 120 bar with diIGSS co-surfactant,*
 117 *[surf] = 0.05 mol dm⁻³, [co-surfactant] = 0.05 mol dm⁻³. w = 5 (open circles, dark green), w = 10 (open down triangles,*
 118 *orange), w = 15 (open squares, blue), w = 20 (open diamonds, pink) and w = 30 (open up triangles, bright green). Fits are to*
 119 *ellipsoid form factor models and are displayed in Figure S 12. Profiles for w10, w15, w20 and w30 have been offset using a*
 120 *scale factor (w10 = x2, w15 = x4, w20 = x8, w30 = x16) for clarity.*

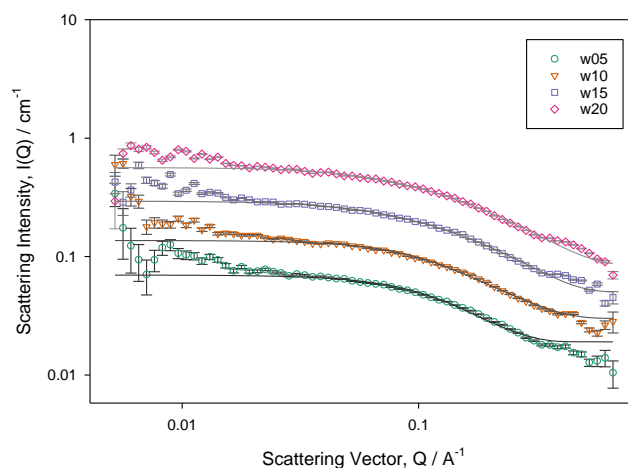


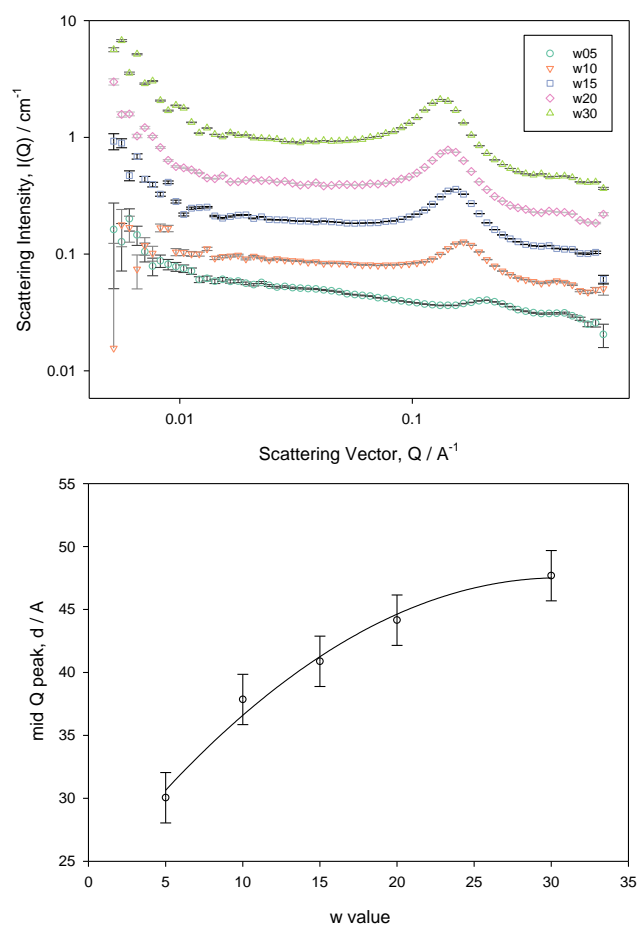
Figure S 11 - HP-SANS profile for hybrid CF₂:SIS1 / water / scCO₂ microemulsions at 120 bar with diIGSS co-surfactant, $[surf] = 0.05 \text{ mol dm}^{-3}$, $[co-surfactant] = 0.05 \text{ mol dm}^{-3}$, $w = 5$ (open circles, green), $w = 10$ (open triangles, orange), $w = 15$ (open squares) and $w = 20$ (open diamonds). Fits are to ellipsoids and are displayed in Figure S 12. Profiles for w_{10} , w_{15} and w_{20} have been offset using a scale factor ($w_{10} = \times 2$, $w_{15} = \times 4$, $w_{20} = \times 8$) for clarity.

surf	w	R Guinier sphere	model	R _a	R _b	Aspect Ratio, J _{mic}
CF2:AOT4	5	26.29	Ellipsoid	25.89	4.72	5.49
	10	24.71		25.24	5.24	4.82
	15	23.34		25.50	5.18	4.92
	20	23.21		25.78	4.62	5.58
	30	23.68		25.40	5.00	5.08
CF2:SIS1	5	24.85	Ellipsoid	26.76	5.34	5.01
	10	28.32		25.79	5.14	5.02
	15	24.57		25.11	5.63	4.46
	20	25.52		24.80	5.38	4.61

Figure S 12 - Parameters obtained from fitting SANS data for w/c microemulsions of hybrid surfactants with DIGSS co-surfactant, $P = 120$ bar, $T = 45^\circ\text{C}$.

surf	Additive	w	model	R / Å	L / Å	Aspect Ratio, J _{mic}
DCF2	C8benz	5	Rods	7.91	60.06	3.80
		10		8.40	67.15	4.00
	C2benz	10	Rods	11.87	97.80	4.12
		15		14.72	158.25	5.38
Hybrid CF2:AOT4		15	Rods	11.32	48.00	2.12

Figure S 13 – Parameters obtained from fitting SANS data for w/c microemulsions of CO_2 —philic surfactants with hydrotropes, $[\text{surf}] = 0.05 \text{ mol dm}^{-3}$, hydrotrope mole fraction, $X = 0.1$, $P = 350$ bar, $T = 45^\circ\text{C}$. Parameters are fit to the form factor for rod-like aggregates.



133

134 *Figure S 14 - HP-SANS profile for CF₂:AOT4 / water / scCO₂ microemulsions at 360 bar with dIGSS co-surfactant, [surf] =*
 135 *0.05 mol dm⁻³, [co-surfactant] = 0.05 mol dm⁻³, w = 5 (open circles), w = 10 (open down triangles), w = 15 (open squares),*
 136 *w = 20 (open diamonds) and w = 30 (open up triangles). Inset - mid-Q peak positions for CF₂:AOT4 / water / scCO₂*
 137 *microemulsion at 360 bar with dIGSS co-surfactant, [surf] = 0.05 mol dm⁻³, [co-surfactant] = 0.05 mol dm⁻³. Profiles for w10,*
 138 *w15, w20 and w30 have been offset using a scale factor (w10 = x2, w15 = x4, w20 = x8, w30 = x16) for clarity.*

139

Estimation of water-in-CO₂ microemulsion viscosities

Relative viscosity can be estimated using Equation S 10³⁻⁵ and Equation S 11⁶.

$$[\eta] \cong 2.5 + 0.4075(J_{mic} - 1)^{1.508}$$

Equation S 10

$$\frac{\eta_{mic}}{\eta_{CO_2}} \cong \eta_{rel} \cong 1 + [\eta]\varphi_p + K_H[\eta]^2\varphi_p^2$$

Equation S 11

K_H is the Huggins coefficient for rods and is in this case ~ 0.4 . For further details please see reference 7.

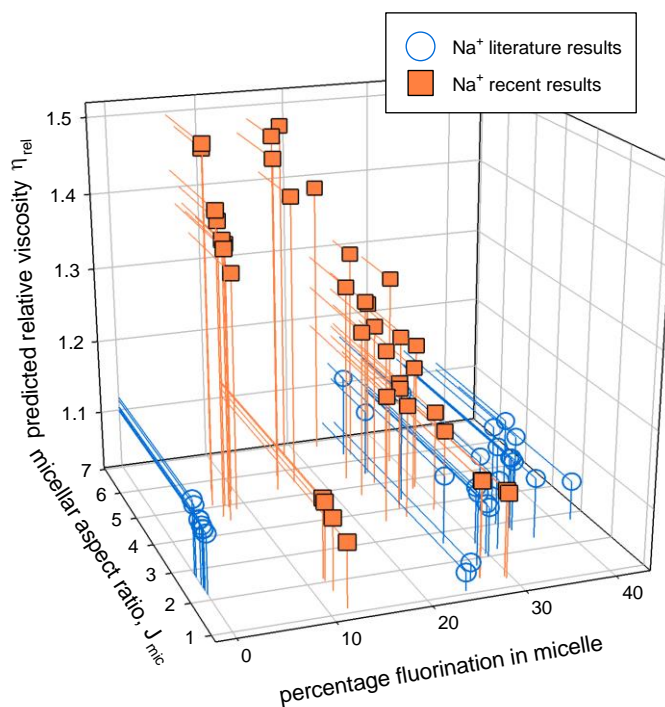


Figure S 15 - Micellar fluorination levels and micellar aspect ratio vs. predicted relative viscosity of all Na⁺ CO₂-philic surfactants reported to generate elongated micelles in scCO₂. Systems introduced in this manuscript are shown as orange filled squares, those in previous research shown as blue circles^{5,8-10}. Micellar volume fraction = $0.012 < \varphi < 0.063$.

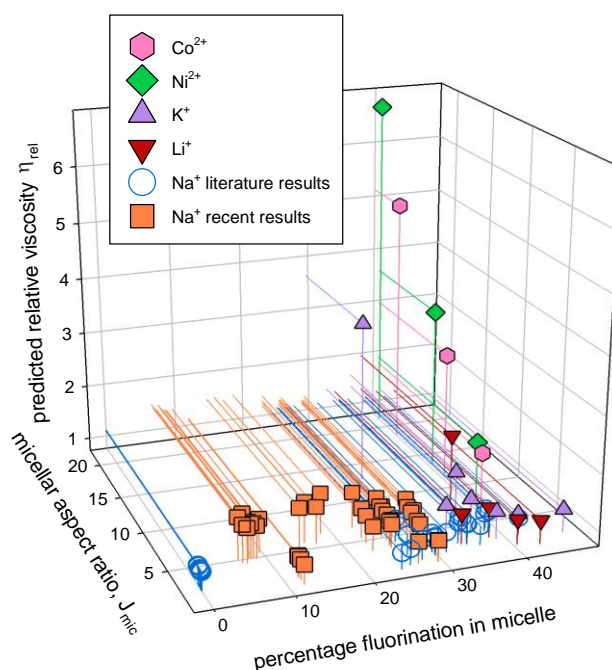


Figure S 16- Micellar fluorination level and aspect ratio vs. relative viscosity of all reported surfactants producing elongated micelles in w/c microemulsions^{4,5,8-11}. Systems introduced in this paper are shown as orange filled squares. Micellar volume fraction = $0.012 < \phi < 0.063$.

References

- (1) SASview version 3.1.2. SASview version 3.1.2 <http://www.sasview.org/>.
- (2) Mohamed, A. PhD Thesis, University of Bristol, 2011.
- (3) Simha, R. The Influence of Brownian Movement on the Viscosity of Solutions. *J. Phys. Chem.* **1940**, *44* (1), 25–34.
- (4) Trickett, K.; Xing, D.; Enick, R. M.; Eastoe, J.; Hollamby, M. J.; Mutch, K. J.; Rogers, S. E.; Heenan, R. K.; Steytler, D. C. Rod-Like Micelles Thicken CO_2 . *Langmuir* **2010**, *26* (6), 83–88.
- (5) Cummings, S.; Xing, D.; Enick, R. M.; Rogers, S. E.; Heenan, R. K.; Grillo, I.; Eastoe, J. Design Principles for Supercritical CO_2 Viscosifiers. *Soft Matter* **2012**, *8* (26), 7044.
- (6) Berry, D. H.; Russel, W. B. The Rheology of Dilute Suspensions of Slender Rods in Weak Flows. *J. Fluid Mech.* **1987**, *180* (1), 475.

- 168 (7) Wierenga, A. M.; Philipse, A. P. Low-Shear Viscosity of Isotropic Dispersions of
169 (Brownian) Rods and Fibres; a Review of Theory and Experiments. *Colloids Surfaces*
170 *A Physicochem. Eng. Asp.* **1998**, *137* (1–3), 355–372.
- 171 (8) James, C.; Hatzopoulos, M. H.; Yan, C.; Smith, G. N.; Alexander, S.; Rogers, S. E.;
172 Eastoe, J. Shape Transitions in Supercritical CO₂ Microemulsions Induced by
173 Hydrotropes. *Langmuir* **2014**, *30* (1), 96–102.
- 174 (9) Yan, C.; Sagisaka, M.; Rogers, S. E.; Hazell, G.; Peach, J.; Eastoe, J. Shape Modification
175 of Water-in-CO₂ Microemulsion Droplets through Mixing of Hydrocarbon and
176 Fluorocarbon Amphiphiles. *Langmuir* **2016**, *32* (6), 1421–1428.
- 177 (10) Sagisaka, M.; Ono, S.; James, C.; Yoshizawa, A.; Mohamed, A.; Guittard, F.; Rogers,
178 S. E.; Heenan, R. K.; Yan, C.; Eastoe, J. Effect of Fluorocarbon and Hydrocarbon Chain
179 Lengths in Hybrid Surfactants for Supercritical CO₂. *Langmuir* **2015**, *31* (27), 7479–
180 7487.
- 181 (11) Consani, K. A.; Smith, R. D. Observations on the Solubility of Surfactants and Related
182 Molecules in Carbon Dioxide at 50°C. *J. Supercrit. Fluids* **1990**, *3* (2), 51–65.

183